Electronic Supplementary Information for

Controlled Reversible Buckling of Polydopamine Spherical Microcapsules: Revealing the Hidden Rich Phenomena of Post-buckling of Spherical Polymeric Shells§

Caifen Lei,[+,1] Qiang Li,[+,1] Lu Yang,[2] Fei Deng,[1] Jianyao Li,[2] Zihan Ye,[1] Ying Wang,*[,1] Zhenkun Zhang*[,1]

1) Key Laboratory of Functional Polymer Materials of Ministry of Education, Institute of Polymer Chemistry, College of Chemistry, Nankai University, 300071 Tianjin, China
2) School of Chemical Engineering and Technology, Tianjin University, Tianjin 300072, China
+ Equal contribution
Email: zkzhang@nankai.edu.cn; wangying79@nankai.edu.cn

§ dedicated to the 100th anniversary of Nankai University

1. 2. THEORY

A homogeneous elastic spherical shells consisting of isotropic materials under an isotropic external compression will initially remain spherical when subjected to compression. When approaching a critical pressure difference (ΔP_c) across the shell wall, the shell undergoes sudden buckling instability and forms an axisymmetric dimple or indentation, in order to avoid energy costing in-plane stretching. ΔP_c has the following relation in terms of the inherent material properties and typical sizes based on the classic thin shell theory,[1]

$$\Delta P_c = \frac{2Y_{3D}}{\sqrt{3(1-\nu^2)}}\left(\frac{T}{R_0}\right)^2 \quad (1)$$

Where Y_{3D} is the three dimensional Yong's modulus, ν is the Poisson's ratio, T is the thickness of the shell and R_0 is the radius of the spherical shell. For a defined shell with fixed material properties such as the shell thickness and radius, this classic theory predicts a constant pressure when buckling occurs. The relative volume variation at this initial buckling due to the external pressure difference ΔP can be expressed as:

$$\left(\frac{\Delta V}{V_0}\right)_{buckle1} = \sqrt{3\left(\frac{1-\nu}{1+\nu}\right)} \times \left(\frac{T}{R_0}\right) \quad (2)$$

The Föppl-von Kármán number γ, which characterizes the order of the magnitude of the ratio between in-plane and out-of plane deformation energies, is the key parameter often used in understanding of the deformation behavior of elastic membranes and shells:

$$\gamma = 12(1-\nu^2)\left(\frac{R_0}{T}\right)^2 \quad (3)$$

It is noted that above theoretic results can only be apply to very small deformation with the depth (H) of the indentation comparable to the shell thickness (T). At this initial deformation, the indentation is has an axisymmetric rim and is exactly the reverse mirror part of the spherical cap. This initial buckling is often refereed as the first buckling stage.

Recent theoretical considerations and numerical simulations have focused on the post buckling stage, where the indentation depth (H) is much higher than the shell thickness with $H \sim 50T$.[2, 3] With the evolution of the buckling, the axisymmetric dimple will turn into a polygonal shape with wrinkles. Quantitative predictions for the critical volume changes at which this transition occurs and the relation of the number of the wrinkle with some material parameters have also been derived.[3] In addition, depending on the deformation rate and the Föppl-von Kármán number, a capsule can buckle following a metastable multi-indented way, during which many dimples will nucleate around the whole surface of a capsules. In the subsequent buckling, these dimples will grow either separately or transit into one indentation.[2] More detailed discussions about these conclusions from theory or simulations will be presented in the main text whenever comparison with experimental results is needed.

2. Supplementary results and figures

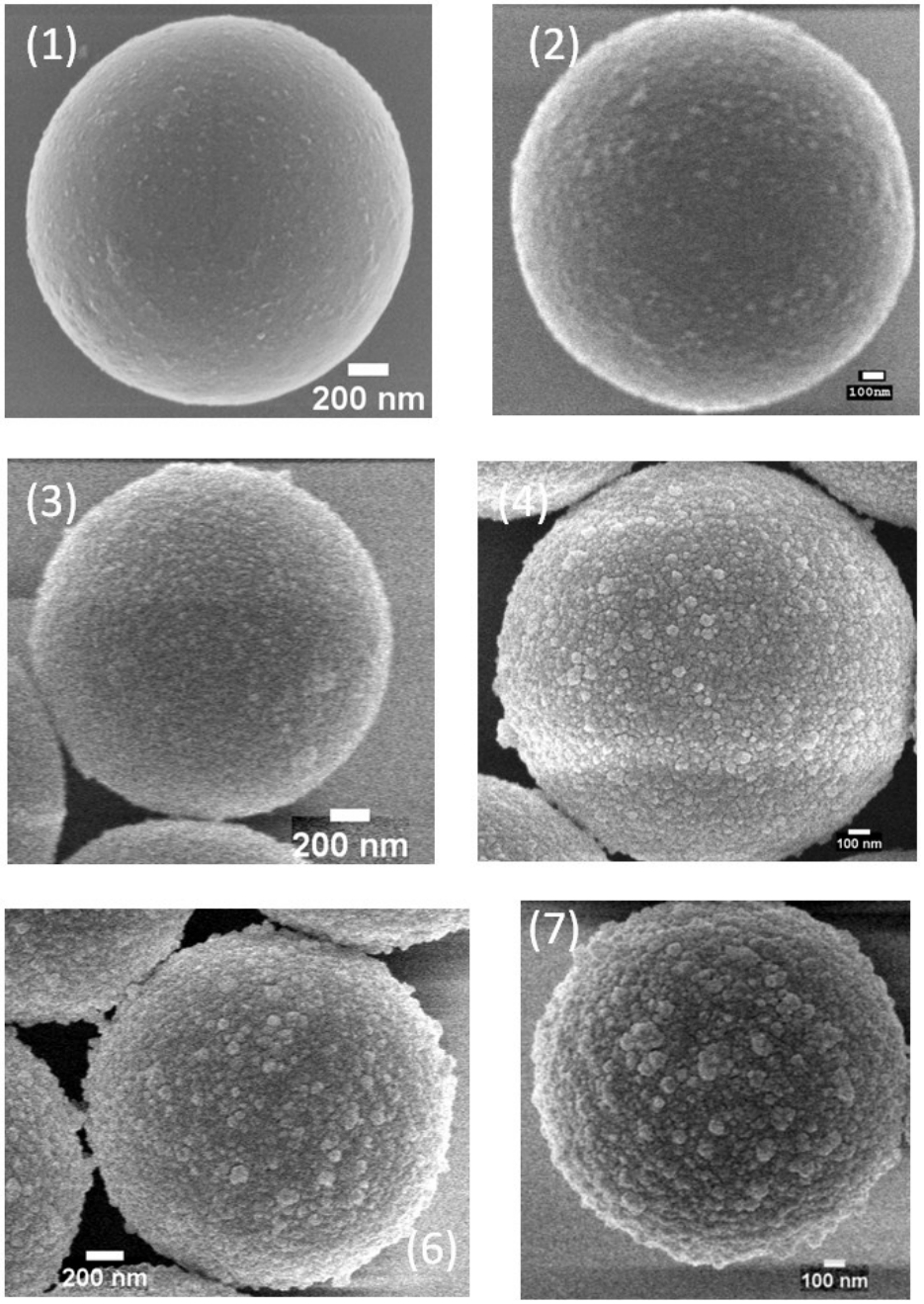

Figure S1. SEM characterization of polydopamine (PDA) coated polystyrene particles through different rounds of stepwise PDA coating. The number in each panel indicates the round of the multiple coating. The coating procedure is described in the main text. The polystyrene particle has a diameter of 1.7 μm.

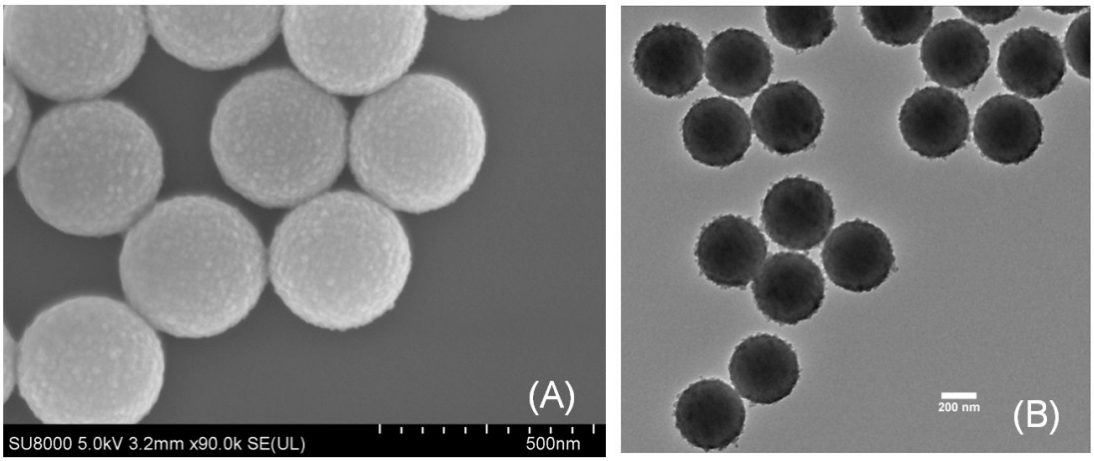

Figure S2. SEM and TEM characterizations of polydopamine coated polystyrene particles with a diameter of around 320 nm.

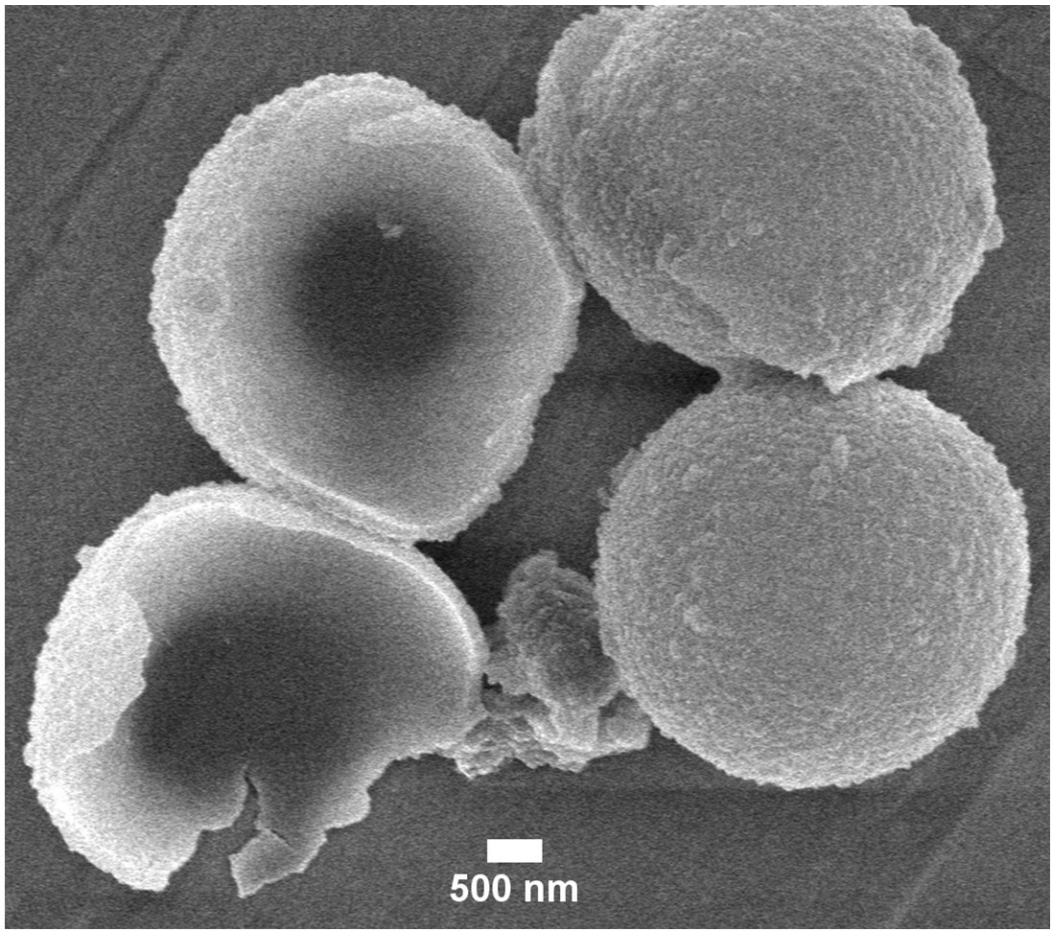

Figure S3. SEM characterization of polydopamine capsules. The broken capsules have a shell with a smooth inner surface and a rough outer surface.

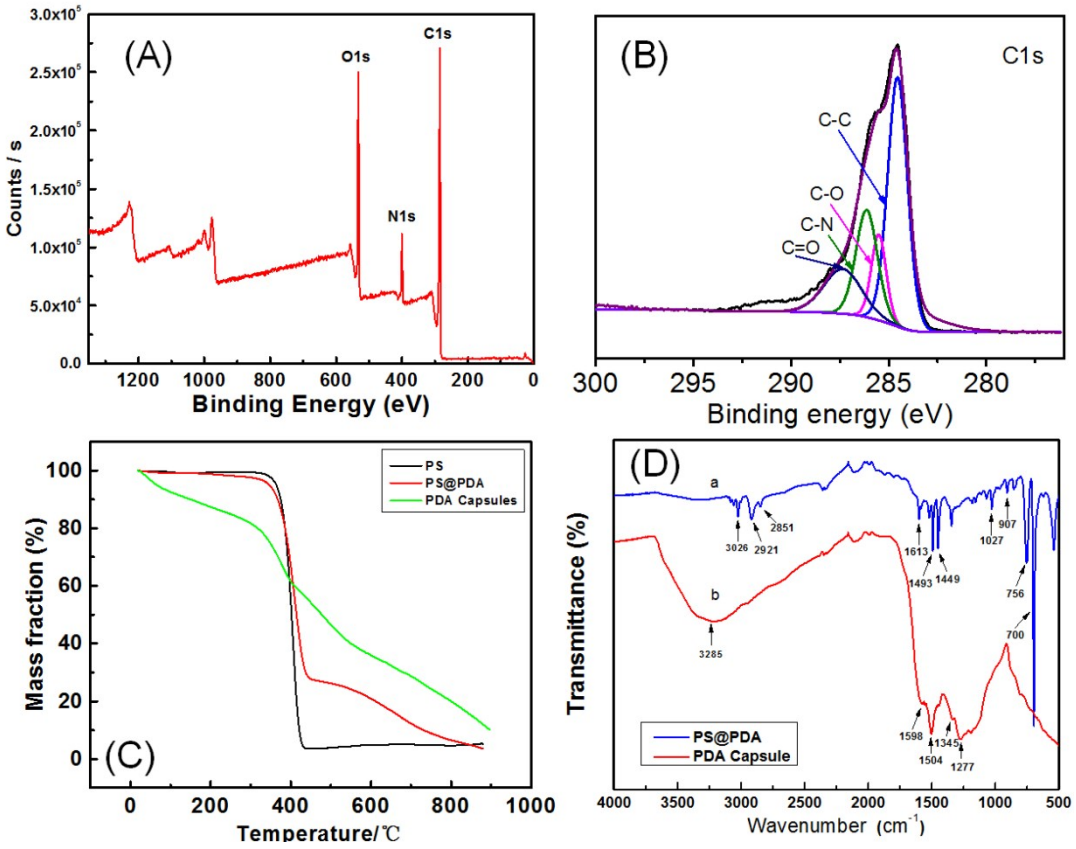

Figure S4. Characterization of PDA capsules by x-ray photoelectron spectroscopy (XPS) (A and B), thermogravimetric analysis (TGA) (C) and infrared spectroscopy (IR) (D). (A) is the XPS survey spectra of the PDA capsules. In (B), the C 1s peak in (A) is deconvoluted into four subpeaks at 284.5eV (C-C/C-H), 285.5eV (C-O), 286.2eV (C-N) and 287.5 eV (C=N), respectively. The peak at 287.5 eV (C=N) can be ascribed to the oxidized intermediate compounds, such as 5,6-indolequinone that exists in the PDA layer. In (C), TGA of PS@PDA hybrid particles have a two-stage decomposition procedure combining pure PS ellipsoids and polydopamine: an initial fast decomposing process in the temperature range of 386 ~ 437 ℃, during which the PS templates decompose completely, together with parts of PDA; After this, a slow procedure up to 800℃ is mainly stems from decomposition of the PDA components. In contrast, the PDA capsules decompose in a wide range of temperature that is typical of pure PDA. Compared to the PS@PDA hybrid particles, the FTIR spectra of the PDA capsules in (D) is similar to that of pure PDA with a peak at 1504 cm^{-1} that is assigned to the C=N vibration modes of the oxidized intermediate compounds of dopamine (*Langmuir* 2013, 29, 8619−8628).

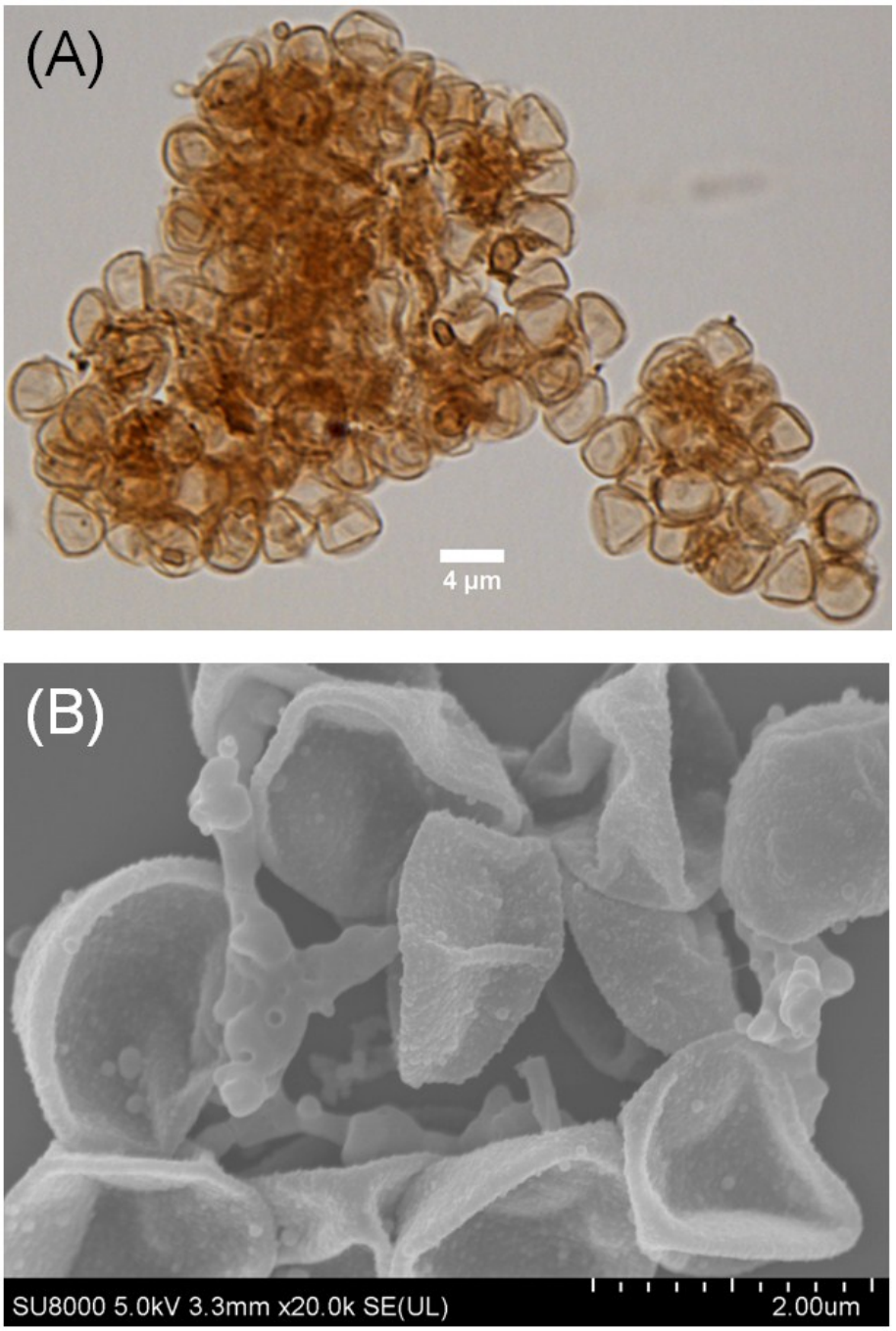

Figure S5. (A) Photo of optical microscopy observation of buckled PDA capsules with a diameter of ca. 4 µm. (B) SEM characterization of buckled PDA capsules with a diameter of 1.7 µm. The samples for both optical microscopy and SEM observations are prepared by directly drying in air one drop of PDA capsule in THF.

2. Supplementary Movies.

Movie S1: Evaporation of THF in the home made optical chamber as shown in Figure 2A of the main text. The evaporation front is parallel to the opening side and moves inward during evaporation. Capsules nearby the approaching evaporation front start to buckle immediately.

Movie S2 and Movie S3: Examples of controlled buckling of PDA capsules into the bowl-like shape with a single indentation as realized by the slow solvent evaporation in the evaporation chamber of Figure 2A in the main text. Serial frames of Movie S2 are also listed in Figure 6 in the main text.

Movie S4: Examples of capsule buckling during which the shape of the indentation rim has a polygonal shape.

Movie S5: Examples of Multi-indented buckling. An isolated suspension of PDA capsules in THF was placed inside the evaporation chamber of Figure 2A. The buckling behaviors of the capsules highlighted by red arrows are also presented in Figure 10 A and B in the main text.

Movie S6: Prebuckled capsules with a deep indention further buckle in the way that a new indentation forms and pushes back the old one. Serial frames of this movie are also presented in Figure 10C of the main text.

Movie S7: Multiple rounds of reversible buckling of PDA capsules by feeding and evaporation of THF in the optical chamber of Figure 2A of the main text.

Movie S8: A capsule swallows an attached PDA particle during buckling into the bowl-like shape. Serial photos from this movie are also listed in Figure 11B of the main text.

References

1. C. Quilliet, *Eur. Phys. J. E*, 2012, **35**, 48.
2. G. A. Vliegenthart and G. Gompper, *New J. Phys.*, 2011, **13**, 045020.
3. S. Knoche and J. Kierfeld, *Eur. Phys. J. E*, 2014, **37**, 62.